


Cite this: *Dalton Trans.*, 2024, **53**, 15465Received 30th May 2024,  
Accepted 29th August 2024

DOI: 10.1039/d4dt01581a

rsc.li/dalton

## Four-step electron transfer coupled spin transition in a cyano-bridged [Fe<sub>2</sub>Co<sub>2</sub>] square complex†

Taisuke Ikeda, Yu-Bo Huang, Shu-Qi Wu,  Wenwei Zheng, Wen-Huang Xu, Xiaopeng Zhang, Tianchi Ji, Mikoto Uematsu, Shinji Kanegawa,  Sheng-Qun Su\* and Osamu Sato \*

The design of molecular functional materials with multi-step magnetic transitions has attracted considerable attention. However, the development of such materials is still infrequent and challenging. Here, a cyano-bridged square Prussian blue complex that exhibits a thermally induced four-step electron transfer coupled spin transition (ETCST) is reported. The magnetic and spectroscopic analyses confirm this multi-step transition. Variable-temperature infrared spectrum suggested the electronic structures in each phase and a four-step transition model is proposed.

### Introduction

Molecular systems that show changes in their stimuli-controllable magnetic properties are promising for functional memory applications, switches, and sensors owing to their microscopic scale and their designability.<sup>1–15</sup> In particular, multi-step magnetic transition has attracted considerable interest, as it would provide additional states for encoding information, which would enable more robust storage devices with higher data density.<sup>16–21</sup> Considering the benefits of molecular materials with multi-step magnetic transitions in high-density storage, several strategies for developing such materials have been proposed. One idea is to adopt molecules or ions that singly provide three or more stable states.<sup>22–31</sup> Cocrystals of multiple switchable components could also be candidates.<sup>32,33</sup> Another strategy is to stabilize and control the packing modes of the molecules by introducing suitable intermolecular interactions.<sup>16–19,34–40</sup> Intermediate (IM) phases are typically formed by symmetry breaking, and they are thermodynamically stabilized by intermolecular interactions; especially hydrogen bonding and  $\pi$ -interactions. In some cases, these interactions provide several IM phases. To develop a molecular system that is capable of multi-step magnetic property change, spin transition systems have been widely studied, as spin transition complexes usually exhibit a reversible change in the spin state of their metal ions in response to

external stimuli such as changes in temperature, pressure, or light, or the presence of certain molecules. A series of Fe(II), Fe(III), Co(II), and Mn(III) complexes with a stimuli-responsive multi-step spin transition have been developed.<sup>17–19,22–27,32,34–37,41–45</sup> In addition, coordination complexes with charge transfer represent a versatile class of molecular materials that could realize multi-step magnetic transitions due to their rich electronic structure that provide multiple accessible oxidation states and spin states.<sup>28,29,46</sup> Such molecular materials include valence tautomeric compounds and Prussian blue analogues (PBAs), where charge transfer occurs between organic ligands and a metal center or between two metal ions.<sup>47–54</sup> For example, a two-step valence tautomerism was recently realized in a dinuclear cobalt complex. In PBA systems, two-step and three-step electron transfer coupled spin transitions (ETCSTs) have been studied based on [Fe<sub>2</sub>Co<sub>2</sub>] square complexes.<sup>16,38–40</sup> Additionally, a four-step transition was achieved in cyano-bridged two-dimensional coordination polymers with the use of spin crossover on their Fe centers.<sup>20,21,55–57</sup>

In this work, we focus on the PBAs that exhibit ETCST to realize a multi-step transition in molecular materials. Because the first discrete molecular PBA that exhibited thermally induced ETCST was reported in a pentanuclear [Co<sub>3</sub>Fe<sub>2</sub>] complex by Dunbar and associates, a number of PBAs, especially [Fe<sub>2</sub>Co<sub>2</sub>] square complexes, have been developed that have exhibited ETCST in response to various stimuli (*e.g.* thermal, light, solvent molecule, pressure and X-ray stimuli).<sup>16,33,38–40,50,58–71</sup> In these complexes, the Fe–CN–Co unit usually forms a Fe<sup>II</sup><sub>LS</sub>–CN–Co<sup>III</sup><sub>LS</sub> diamagnetic state in the low-temperature (LT) phase and a Fe<sup>III</sup><sub>LS</sub>–CN–Co<sup>II</sup><sub>HS</sub> paramagnetic state in the high-temperature (HT) phase *via* reversible spin crossover on the Co center and electron transfer from Co(II) to Fe(III) (Fig. 1).

Institute for Materials Chemistry and Engineering and IRCCS, Kyushu University, 744 Motoooka, Nishi-ku, Fukuoka 819-0395, Japan. E-mail: sato@cm.kyushu-u.ac.jp, s-su@cm.kyushu-u.ac.jp

† Electronic supplementary information (ESI) available. CCDC 2337773. For ESI and crystallographic data in CIF or other electronic format see DOI: <https://doi.org/10.1039/d4dt01581a>

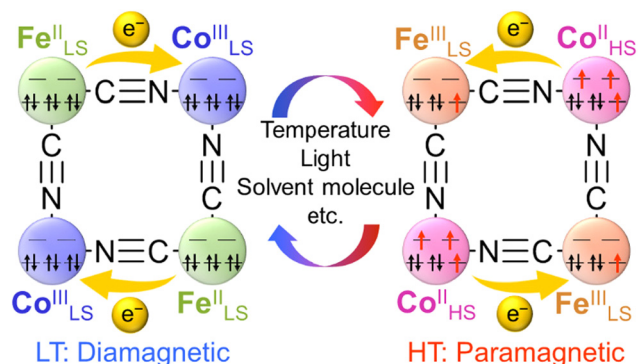


Fig. 1 Typical ETCST process in a cyano-bridged  $[\text{Fe}_2\text{Co}_2]$  square unit.

In this study, a new cyano-bridged  $[\text{Fe}_2\text{Co}_2]$  complex,  $\{[\text{Fe}(\text{Tp})(\text{CN})_3]_2[\text{Co}(\text{L})_2](\text{ClO}_4)_2 \cdot 8\text{EtOH}$  (**1**·8EtOH, Tp: hydrotris(pyrazol-1-yl)borate, L: *N,N'*-bis(4-methylbenzyl)-*N,N'*-bis(pyridine-2-ylmethyl)ethane-1,2-diamine), is synthesized and characterized by single-crystal X-ray diffraction analysis, magnetic susceptibility measurement, variable-temperature infrared (IR) spectroscopy, and UV-vis spectroscopy. Our study reveals that **1** exhibits thermally induced four-step ETCST, which is currently being explored but has rarely been reported, as well as photo-induced ETCST induced by desolvation.

## Results and discussion

### Synthetic procedure and crystallography

**1**·8EtOH was prepared *via* the reaction of  $\text{Co}(\text{ClO}_4)_2 \cdot 6\text{H}_2\text{O}$ , L and  $[\text{NBu}_4][\text{Fe}(\text{Tp})(\text{CN})_3]$  in ethanol. The purity of the product was confirmed by powder X-ray diffraction analysis (Fig. S1†). Subsequently, **1** was obtained by heating **1**·8EtOH at 400 K in nitrogen atmosphere for 1 hour.

The single-crystal X-ray diffraction analysis of **1**·8EtOH was performed at 100 K (Fig. 2). **1**·8EtOH was observed to crystallize in the monoclinic  $P2_1/n$  space group. In one crystallographic asymmetric unit, half of the square core was composed of a  $[\text{FeCo}]$  unit, one perchlorate as counter anion, and four ethanol molecules as the crystal solvent. The Fe center was coordinated to three N atoms from the Tp ligand and three C atoms from cyanides to form a  $\text{C}_3\text{N}_3$  distorted octa-

hedral coordination environment. However, the Co center was coordinated to four N atoms by the ligand L, and the other two coordination sites were occupied by two N atoms of cyanide bridging from the  $[\text{Fe}(\text{Tp})(\text{CN})_3]$  unit to form the  $\text{N}_6$  coordination environment. The average of the length of the bonds between  $\text{Fe}-\text{C}_{\text{bridge}}$ ,  $\text{Fe}-\text{C}_{\text{terminal}}$  and  $\text{Fe}-\text{N}$  were 1.863, 1.905, and 2.002 Å, whereas those of  $\text{Co}-\text{N}_{\text{cyanide}}$ ,  $\text{Co}-\text{N}_{\text{amine}}$ , and  $\text{Co}-\text{N}_{\text{aromatic}}$  were 1.884, 1.996, and 1.954 Å, respectively. These values are characteristic of the  $\text{Fe}_{\text{LS}}^{\text{II}}$  and  $\text{Co}_{\text{LS}}^{\text{III}}$  states.<sup>16,33,38–40,50,59–71</sup> The packing structure of **1**·8EtOH at 100 K was shown in Fig. S2.† Unfortunately, the crystal structure after desolvation could not be obtained due to the cracking of the crystal.

### Magnetic study

The magnetic susceptibility of **1**·8EtOH, and **1** before and after irradiation measured in the temperature range of 5–400 K (Fig. 3a). **1**·8EtOH demonstrated a diamagnetic character in the temperature range of 5–295 K, which indicated a  $[\text{Fe}_{\text{LS}}^{\text{II}}(S=0)_2\text{Co}_{\text{LS}}^{\text{III}}(S=0)_2]$  electronic structure. As the temperature further increased, the  $\chi_{\text{M}}T$  value abruptly increased and reached  $7.42 \text{ cm}^3 \text{ K mol}^{-1}$  at temperatures above 370 K, which is a typical value of a paramagnetic  $[\text{Fe}_{\text{LS}}^{\text{III}}(S=1/2)_2\text{Co}_{\text{HS}}^{\text{II}}(S=3/2)_2]$  structure.<sup>16,33,38–40,50,59–71</sup> This  $\chi_{\text{M}}T$  value is larger than the spin-only value ( $4.5 \text{ cm}^3 \text{ K mol}^{-1}$ ), which suggests that there is an orbital contribution to the magnetic moment. This means that the ETCST may occur here along with the loss of solvent (see the ESI†).

For **1**, however, the  $\chi_{\text{M}}T$  value changed gradually in the temperature range of 160–360 K with a multi-step transition. At a temperature below 160 K, a constant  $\chi_{\text{M}}T$  value of  $0.76 \text{ cm}^3 \text{ K mol}^{-1}$  was observed, which suggests a diamagnetic  $[\text{Fe}_{\text{LS}}^{\text{II}}\text{Co}_{\text{LS}}^{\text{III}}]$  structure with a slight residual of paramagnetic  $[\text{Fe}_{\text{LS}}^{\text{III}}\text{Co}_{\text{HS}}^{\text{II}}]$  structure. During the heating process, plateaus were observed at 203, 245, and 295 K, which demonstrated  $\chi_{\text{M}}T$  values of 2.34, 3.84, and  $5.21 \text{ cm}^3 \text{ K mol}^{-1}$ , respectively (Fig. 3b). At temperatures above 360 K, the  $\chi_{\text{M}}T$  value reached  $7.42 \text{ cm}^3 \text{ K mol}^{-1}$ . The multi-step character was also observed during the cooling process. The magnetic susceptibility curves are reproducible, even with different temperature sweeping rates (Fig. S6 and S7†). According to the first derivative of the  $\chi_{\text{M}}T$  vs.  $T$  curve in the heating process, this transition is a four-step transition, which has rarely been reported for molecular systems, especially for PBAs (Fig. 3c). These data reveal that **1** exhibits thermally induced ETCST from the  $[\text{Fe}_{\text{LS}}^{\text{II}}\text{Co}_{\text{LS}}^{\text{III}}]$  to the  $[\text{Fe}_{\text{LS}}^{\text{III}}\text{Co}_{\text{HS}}^{\text{II}}]$  state *via* three IM phases.

In addition, to investigate the light-induced magnetic susceptibility of the present complexes, **1** was set to 5 K and irradiated with green light (532 nm). The  $\chi_{\text{M}}T$  value increased from  $1.09 \text{ cm}^3 \text{ K mol}^{-1}$  to  $7.15 \text{ cm}^3 \text{ K mol}^{-1}$ , which indicates a conversion from a ground state to a photo-induced metastable state *via* ETCST. During the heating process, the metastable state completely relaxed to the ground state that demonstrates an  $\chi_{\text{M}}T$  value of  $0.71 \text{ cm}^3 \text{ K mol}^{-1}$  at 150 K.

Interestingly, the thermally induced transition disappeared again on the exposure to air of **1** (Fig. S8†). A thermogravimetric analysis and an elemental analysis suggested the

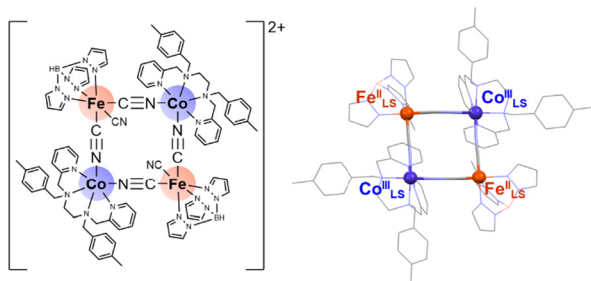
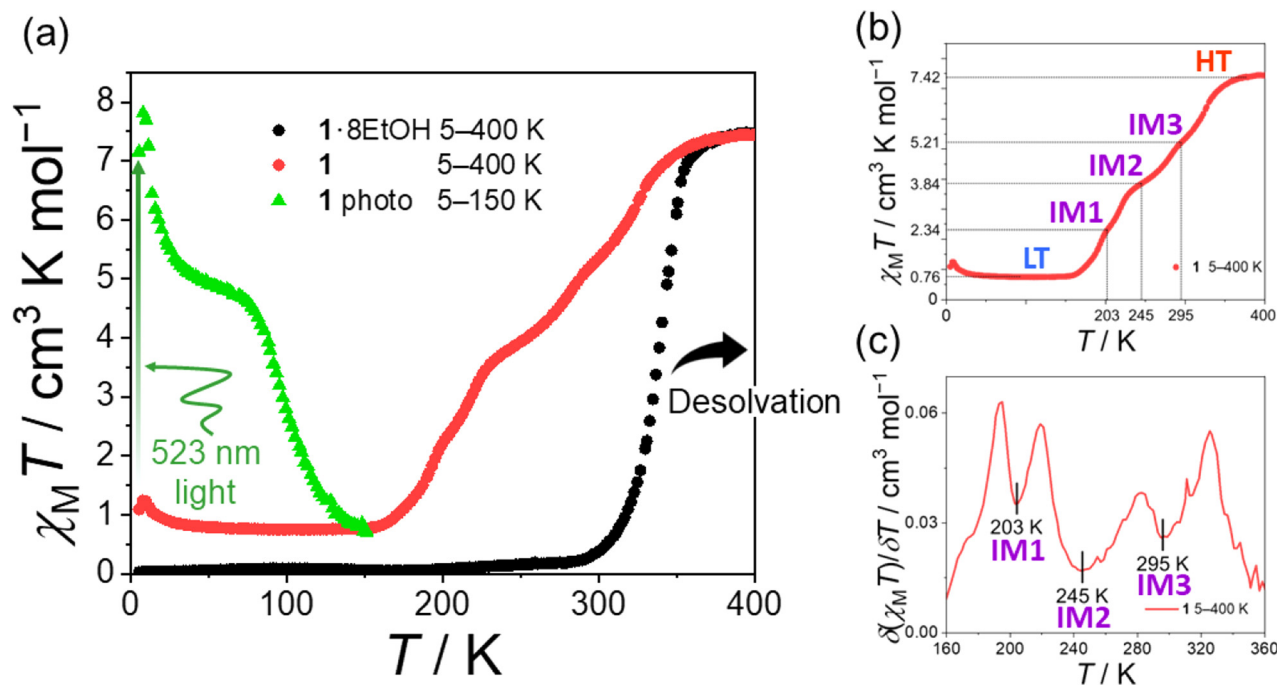


Fig. 2 Chemical structure (left) and crystal structure (right) of **1**·8EtOH at 100 K. Counter anions and solvent molecules were omitted for clarity.



**Fig. 3** (a) Magnetic susceptibilities of 1·8EtOH (black circle), 1 (red circle), and photo irradiated 1 (green triangle). The sweeping rates are 5 K min<sup>-1</sup> for all measurements. (b) Magnetic susceptibility of 1 (taken from (a)). (c) The first derivative of the  $\chi_M T$  vs.  $T$  curve of 1.

solvation of water occurred to form 1·3H<sub>2</sub>O (Fig. S5†). That means that the ETCST phenomenon was turned on/off by desolvation/solvation.

#### Variable-temperature IR spectroscopy

As we know, there are two possible mechanisms for multi-step ETCST in the [Fe<sub>2</sub>Co<sub>2</sub>] unit. One is that ETCST occurs antecedently at only one [FeCo] site, followed by the other site, to

form a [Fe<sup>II</sup><sub>LS</sub>Co<sup>III</sup><sub>LS</sub>Fe<sup>III</sup><sub>LS</sub>Co<sup>II</sup><sub>HS</sub>] unit in the IM phase (Fig. 4a(I)). Another is that ETCST occurs at two [FeCo] sites at the same time, which changes the ratio of the [(Fe<sup>II</sup><sub>LS</sub>Co<sup>III</sup><sub>LS</sub>)<sub>2</sub>] and [(Fe<sup>III</sup><sub>LS</sub>Co<sup>II</sup><sub>HS</sub>)<sub>2</sub>] states (Fig. 4a(II)). To investigate the mechanism of this four-step ETCST, variable-temperature IR spectroscopy was carried out (Fig. 4b).

For complex 1, absorption peaks at 80 K was observed in the range of 2070–2130 cm<sup>-1</sup>. These peaks belong to the

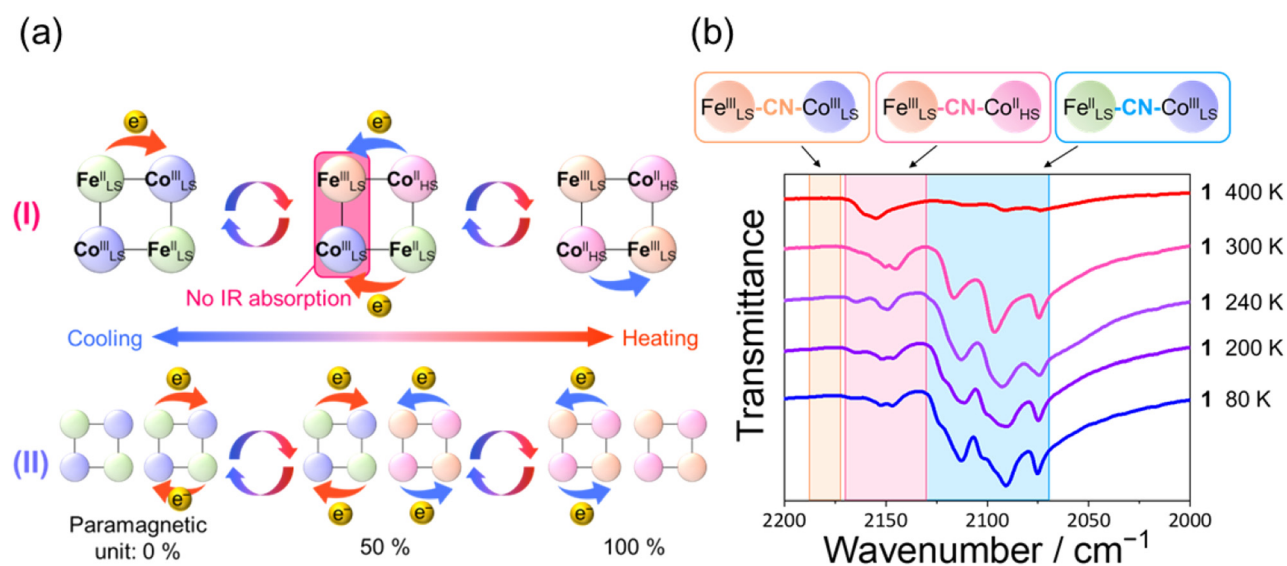


**Fig. 4** (a) Two kinds of ETCST mechanisms in a [Fe<sub>2</sub>Co<sub>2</sub>] unit. Combined with IR spectrum, simultaneous ETCST; mechanism(ii) is reasonable. (b) Variable-temperature IR spectrum of 1.

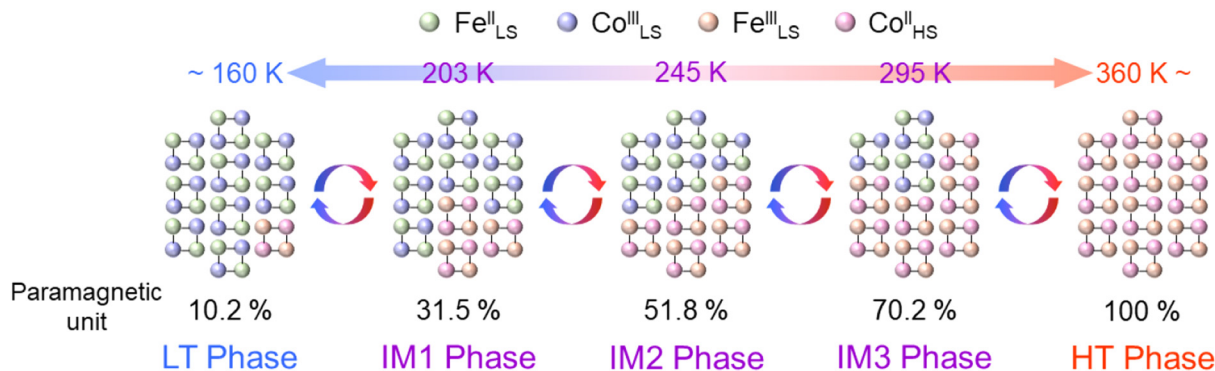


Fig. 5 Schematic diagram of four-step transition.

cyanide stretching modes in the  $\text{Fe}_{\text{LS}}^{\text{II}}\text{-CN-Co}_{\text{LS}}^{\text{III}}$  structure.<sup>16,33,38–40,50,59–67</sup> In addition, another peak was observed at 2130–2170  $\text{cm}^{-1}$ , which is the typical absorption of the  $\text{Fe}_{\text{LS}}^{\text{III}}\text{-CN-Co}_{\text{HS}}^{\text{II}}$  structure.<sup>16,33,38–40,50,59–67</sup> This spectrum means **1** is composed of both  $[\text{Fe}_{\text{LS}}^{\text{II}}\text{Co}_{\text{LS}}^{\text{III}}]$  and  $[\text{Fe}_{\text{LS}}^{\text{III}}\text{Co}_{\text{HS}}^{\text{II}}]$  structures in LT phase. However, the peak in the region 2070–2130  $\text{cm}^{-1}$  became weaker during the heating process. Contrarily, the peak at 2130–2170  $\text{cm}^{-1}$  became stronger. This spectral change indicates that the change in temperature induced ETCST in **1**.

Moreover, there was no peak around 2180  $\text{cm}^{-1}$ , which is characteristic of the  $\text{Fe}_{\text{LS}}^{\text{III}}\text{-CN-Co}_{\text{LS}}^{\text{III}}$  structure.<sup>72–76</sup> This spectral absence suggests that there was no  $[\text{Fe}_{\text{LS}}^{\text{II}}\text{Co}_{\text{LS}}^{\text{III}}\text{Fe}_{\text{LS}}^{\text{III}}\text{Co}_{\text{HS}}^{\text{II}}]$  unit in any phase, and that the four-step transition can be described by changing the ratio of  $[\text{Fe}_{\text{LS}}^{\text{II}}\text{Co}_{\text{LS}}^{\text{III}}]$  and  $[\text{Fe}_{\text{LS}}^{\text{III}}\text{Co}_{\text{HS}}^{\text{II}}]$  units as shown in Fig. 4a(II). A schematic of such a four-step transition is illustrated in Fig. 5.

Although the crystal structure of **1** could not be obtained, the mechanism of the four-step transition was proposed as related to previously reported cases. Considering the reason why the IM states were stabilized, two possibilities were proposed. The first is that a crystallographically non-equivalent  $[\text{Fe}_2\text{Co}_2]$  unit was generated *via* desolvation. In the whole structure of **1**·8EtOH, due to the ethanol molecules occupying part of volume, the desolvation may destroy the original stacking of  $[\text{Fe}_2\text{Co}_2]$  units. The second is that the symmetry breaking that occurred was supported by intermolecular interaction. Strong intermolecular interaction such as  $\pi$ -interaction or hydrogen bonding can thermodynamically stabilize the IM phases. In particular, the ligand on Co contains flexible 4-methylbenzyl groups that may create  $\pi$ -interactions. In any case, the packing structure should have changed when the ethanol molecules completely left *via* heating at 400 K, and this would trigger multi-step behavior.

## Conclusions

Thermally induced four-step ETCST, which is a multi-step transition that is rarely reported in molecular systems, was observed in a cyano-bridged  $[\text{Fe}_2\text{Co}_2]$  square complex **1**.

Additionally, **1** exhibited photo-induced ETCST also, and these transitions were turned on/off by desolvation/solvation. The mechanism of such a four-step ETCST was confirmed through variable-temperature IR spectroscopy. This result indicated that the four-step transition was achieved by changing the ratio of the  $[\text{Fe}_{\text{LS}}^{\text{II}}\text{Co}_{\text{LS}}^{\text{III}}]_2$  and  $[\text{Fe}_{\text{LS}}^{\text{III}}\text{Co}_{\text{HS}}^{\text{II}}]_2$  units. This work provides a novel multi-step transition system for the development of high-density molecular devices.

## Author contributions

O. S. and S.-Q. S. supervised the project. T. I., Y.-B. H., M. U., T. J., X. Z., S.-Q. W. and S.-Q. S. carried out synthetic and crystallographic experiments. Magnetometries were performed by T. I., S.-Q. W., S. K. and S.-Q. S. T. I., W. Z., W.-H. X. and S.-Q. S. performed spectroscopic measurements. T. I., S.-Q. W., S.-Q. S. and O. S. discussed and co-wrote the manuscript.

## Data availability

The authors confirm that the data supporting the findings of this study are available within the article and its ESI.† Supplementary information (ESI) available: IR spectra, UV spectra, TG curves, powder X-ray diffraction data and magnetic studies. Crystallographic data for compound **1**·8EtOH was deposited at the Crystallographic Data Center with CCDC number 2337773.

## Conflicts of interest

The authors declare no competing financial interests.

## Acknowledgements

This work was supported by JSPS KAKENHI (24H00466 and 24K17698). This work was supported by the MEXT Project of “Integrated Research Consortium on Chemical Sciences”.

S.-Q. W. are grateful for the support by Iketani Science and Technology Foundation (0351039A).

## References

- O. Kahn and C. J. Martinez, *Science*, 1998, **279**, 44–48.
- A. Bousseksou, G. Molnár and G. Matouzenko, *Eur. J. Inorg. Chem.*, 2004, 4353–4369.
- O. Sato, J. Tao and Y. Z. Zhang, *Angew. Chem., Int. Ed.*, 2007, **46**, 2152–2187.
- D. Aguilà, Y. Prado, E. S. Koumoussi, C. Mathonière and R. Clérac, *Chem. Soc. Rev.*, 2016, **45**, 203–224.
- O. Sato, *Nat. Chem.*, 2016, **8**, 644–656.
- Y.-S. Meng, O. Sato and T. Liu, *Angew. Chem., Int. Ed.*, 2018, **57**, 12216–12226.
- P. Sadhukhan, S. Q. Wu, J. I. Long, T. Nakanishi, S. Kanegawa, K. G. Gao, K. Yamamoto, H. Okajima, A. Sakamoto, M. L. Baker, T. Kroll, D. Sokaras, A. Okazawa, N. Kojima, Y. Shiota, K. Yoshizawa and O. Sato, *Nat. Commun.*, 2021, **12**, 4836.
- M. Seredyuk, K. Znojnyak, F. J. Valverde-Munoz, I. da Silva, M. C. Muñoz, Y. S. Moroz and J. A. Real, *J. Am. Chem. Soc.*, 2022, **144**, 14297–14309.
- S. G. Wu, L. F. Wang, Z. Y. Ruan, S. N. Du, S. Gómez-Coca, Z. P. Ni, E. Ruiz, X. M. Chen and M. L. Tong, *J. Am. Chem. Soc.*, 2022, **144**, 14888–14896.
- S. Q. Su, S. Q. Wu, Y. B. Huang, W. H. Xu, K. G. Gao, A. Okazawa, H. Okajima, A. Sakamoto, S. Kanegawa and O. Sato, *Angew. Chem., Int. Ed.*, 2022, **61**, e202208771.
- X. P. Zhang, W. H. Xu, W. W. Zheng, S. Q. Su, Y. B. Huang, Q. R. Shui, T. C. Ji, M. Uematsu, Q. Chen, M. Tokunaga, K. G. Gao, A. Okazawa, S. Kanegawa, S. Q. Wu and O. Sato, *J. Am. Chem. Soc.*, 2023, **145**, 15647–15651.
- S. Q. Su, S. Q. Wu, S. Kanegawa, K. Yamamoto and O. Sato, *Chem. Sci.*, 2023, **14**, 10631–10643.
- G. Z. Huang, Y. S. Xia, F. Yang, W. J. Long, J. J. Liu, J. P. Liao, M. Zhang, J. Liu and Y. Q. Lan, *J. Am. Chem. Soc.*, 2023, **145**, 26863–26870.
- Y. Y. Wu, Z. Y. Li, S. Peng, Z. Y. Zhang, H. M. Cheng, H. Su, W. Q. Hou, F. L. Yang, S. Q. Wu, O. Sato, J. W. Dai, W. Li and X. H. Bu, *J. Am. Chem. Soc.*, 2024, **146**, 8206–8215.
- F. Yin, J. Yang, L. P. Zhou, X. Meng, C. B. Tian and Q. F. Sun, *J. Am. Chem. Soc.*, 2024, **146**, 7811–7821.
- M. Nihei, Y. Yanai, I. J. Hsu, Y. Sekine and H. Oshio, *Angew. Chem., Int. Ed.*, 2017, **56**, 591–594.
- H. Hagiwara, R. Minoura, T. Udagawa, K. Mibu and J. Okabayashi, *Inorg. Chem.*, 2020, **59**, 9866–9880.
- A. Orellana-Silla, F. J. Valverde-Muñoz, M. C. Muñoz, C. Bartual-Murgui, S. Ferrer and J. A. Real, *Inorg. Chem.*, 2022, **61**, 4484–4493.
- Y. Y. Wu, S. Peng, Z. Y. Zhang, Y. Gao, G. Y. Xu, J. W. Dai, Z. Y. Li and M. Yamashita, *Chin. J. Chem.*, 2024, **42**, 879–886.
- D. J. Mondal, A. Mondal, A. Paul and S. Konar, *Inorg. Chem.*, 2022, **61**, 4572–4580.
- S. G. Wu, S. Bala, Z. Y. Ruan, G. Z. Huang, Z. P. Ni and M. L. Tong, *Chin. Chem. Lett.*, 2022, **33**, 1381–1384.
- J. A. Real, H. Bolvin, A. Bousseksou, A. Dworkin, O. Kahn, F. Varret and J. Zarembowitch, *J. Am. Chem. Soc.*, 1992, **114**, 4650–4658.
- J. F. Létard, J. A. Real, N. Moliner, A. B. Gaspar, L. Capes, O. Cador and O. Kahn, *J. Am. Chem. Soc.*, 1999, **121**, 10630–10631.
- R. Clérac, F. A. Cotton, K. R. Dunbar, T. B. Lu, C. A. Murillo and X. P. Wang, *J. Am. Chem. Soc.*, 2000, **122**, 2272–2278.
- R. J. Wei, Q. Huo, J. Tao, R. B. Huang and L. S. Zheng, *Angew. Chem., Int. Ed.*, 2011, **50**, 8940–8943.
- T. Matsumoto, G. N. Newton, T. Shiga, S. Hayami, Y. Matsui, H. Okamoto, R. Kumai, Y. Murakami and H. Oshio, *Nat. Commun.*, 2014, **5**, 3865.
- W. Wen, Y. S. Meng, C. Q. Jiao, Q. Liu, H. L. Zhu, Y. M. Li, H. Oshio and T. Liu, *Angew. Chem., Int. Ed.*, 2020, **59**, 16393–16397.
- G. K. Gransbury, B. N. Livesay, J. T. Janetzki, M. A. Hay, R. W. Gable, M. P. Shores, A. Starikova and C. Boskovic, *J. Am. Chem. Soc.*, 2020, **142**, 10692–10704.
- C. Lecourt, Y. Izumi, L. Khrouz, F. Toche, R. Chiriac, N. Bélanger-Desmarais, C. Reber, O. Fabelo, K. Inoue, C. Desroches and D. Luneau, *Dalton Trans.*, 2020, **49**, 15646–15662.
- C. Y. Zheng, S. W. Jia, Y. B. Dong, J. P. Xu, H. H. Sui, F. Wang and D. F. Li, *Inorg. Chem.*, 2019, **58**, 14316–14324.
- K. C. Khadanand, T. Woods and L. Olshansky, *Angew. Chem., Int. Ed.*, 2023, **62**, e202311790.
- B. Li, R. J. Wei, J. Tao, R. B. Huang, L. S. Zheng and Z. P. Zheng, *J. Am. Chem. Soc.*, 2010, **132**, 1558–1566.
- L. Y. Meng, Y. F. Deng, S. M. Holmes and Y. Z. Zhang, *Dalton Trans.*, 2023, **52**, 1616–1622.
- S. Hayami, Z. Z. Gu, H. Yoshiki, A. Fujishima and O. Sato, *J. Am. Chem. Soc.*, 2001, **123**, 11644–11650.
- Z. Y. Li, J. W. Dai, Y. Shiota, K. Yoshizawa, S. Kanegawa and O. Sato, *Chem. – Eur. J.*, 2013, **19**, 12948–12952.
- E. Dobbelaar, V. B. Jakobsen, E. Trzop, M. Lee, S. Chikara, X. X. Ding, H. Müller-Bunz, K. Esien, S. Felton, M. A. Carpenter, E. Collet, G. G. Morgan and V. S. Zapf, *Angew. Chem., Int. Ed.*, 2022, **61**, e202114021.
- V. B. Jakobsen, E. Trzop, E. Dobbelaar, L. C. Gavin, S. Chikara, X. X. Ding, M. Lee, K. Esien, H. Müller-Bunz, S. Felton, E. Collet, M. A. Carpenter, V. S. Zapf and G. G. Morgan, *J. Am. Chem. Soc.*, 2022, **144**, 195–211.
- M. Nihei, Y. Sekine, N. Suganami, K. Nakazawa, A. Nakao, H. Nakao, Y. Murakami and H. Oshio, *J. Am. Chem. Soc.*, 2011, **133**, 3592–3600.
- S. Kamilya, S. Ghosh, Y. L. Li, P. Dechambenoit, M. Rouzières, R. Lescouëzec, S. Mehta and A. Mondal, *Inorg. Chem.*, 2020, **59**, 11879–11888.
- S. Kamilya, S. Ghosh, S. Mehta and A. Mondal, *J. Phys. Chem. A*, 2021, **125**, 4775–4783.
- N. F. Sciortino, K. R. Scherl-Gruenwald, G. Chastanet, G. J. Halder, K. W. Chapman, J. F. Létard and C. J. Kepert, *Angew. Chem., Int. Ed.*, 2012, **51**, 10154–10158.

- 42 J. Yuan, S. Q. Wu, M. J. Liu, O. Sato and H. Z. Kou, *J. Am. Chem. Soc.*, 2018, **140**, 9426–9433.
- 43 H. Douib, L. Cornet, J. F. Gonzalez, E. Trzop, V. Dorcet, A. Gouasmia, L. Ouahab, O. Cadour and F. Pointillart, *Eur. J. Inorg. Chem.*, 2018, 4452–4457.
- 44 N. G. Spitsyna, M. A. Blagov, V. A. Lazarenko, R. D. Svetogorov, Y. V. Zubavichus, L. V. Zorina, O. Maximova, S. A. Yaroslavtsev, V. S. Rusakov, G. V. Raganyan, E. B. Yagubskii and A. N. Vasiliev, *Inorg. Chem.*, 2021, **60**, 17462–17479.
- 45 J. P. Xue, Y. Hu, B. Zhao, Z. K. Liu, J. Xie, Z. S. Yao and J. Tao, *Nat. Commun.*, 2022, **13**, 3510.
- 46 O. S. Jung, Y. A. Lee, S. H. Park, Y. J. Kim, K. H. Yoo and D. C. Kim, *Bull. Chem. Soc. Jpn.*, 2001, **74**, 305–309.
- 47 S. Kanegawa, Y. Shiota, S. Kang, K. Takahashi, H. Okajima, A. Sakamoto, T. Iwata, H. Kandori, K. Yoshizawa and O. Sato, *J. Am. Chem. Soc.*, 2016, **138**, 14170–14173.
- 48 S. Q. Wu, M. J. Liu, K. G. Gao, S. Kanegawa, Y. Horie, G. Aoyama, H. Okajima, A. Sakamoto, M. L. Baker, M. S. Huzan, P. Bencok, T. Abe, Y. Shiota, K. Yoshizawa, W. H. Xu, H. Z. Kou and O. Sato, *Nat. Commun.*, 2020, **11**, 1992.
- 49 M. Cammarata, S. Zerdane, L. Balducci, G. Azzolina, S. Mazerat, C. Exertier, M. Trabuco, M. Levantino, R. Alonso-Mori, J. M. Glowina, S. Song, L. Catala, T. Mallah, S. F. Matar and E. Collet, *Nat. Chem.*, 2021, **13**, 10–14.
- 50 J. Yadav, D. J. Mondal and S. Konar, *Chem. Commun.*, 2021, 57, 5925–5928.
- 51 P. Sadhukhan, S. Q. Wu, S. Kanegawa, S. Q. Su, X. P. Zhang, T. Nakanishi, J. I. Long, K. G. Gao, R. Shimada, H. Okajima, A. Sakamoto, J. G. Chiappella, M. S. Huzan, T. Kroll, D. Sokaras, M. L. Baker and O. Sato, *Nat. Commun.*, 2023, **14**, 3394.
- 52 E. Hruska, Q. S. Zhu, S. Biswas, M. T. Fortunato, D. R. Broderick, C. M. Morales, J. M. Herbert, C. Turro and L. R. Baker, *J. Am. Chem. Soc.*, 2024, **146**, 8031–8042.
- 53 K. K. Yao, C. W. Dong, K. Y. Cao, Y. Zhang and S. Yang, *Adv. Funct. Mater.*, 2024, 2313938.
- 54 S. Kanegawa, S. Q. Wu, Z. Q. Zhou, Y. Shiota, T. Nakanishi, K. Yoshizawa and O. Sato, *J. Am. Chem. Soc.*, 2024, **146**, 11553–11561.
- 55 F. J. Valverde-Muñoz, C. Bartual-Murgui, L. Piñeiro-López, M. C. Muñoz and J. A. Real, *Inorg. Chem.*, 2019, **58**, 10038–10046.
- 56 L. Piñeiro-López, F. J. Valverde-Muñoz, E. Trzop, M. C. Muñoz, M. Seredyuk, J. Castells-Gil, I. da Silva, C. Martí-Gastaldo, E. Collet and J. A. Real, *Chem. Sci.*, 2021, **12**, 1317–1326.
- 57 O. I. Kucheriv, S. I. Shylin, V. Y. Sirenko, V. Ksenofontov, W. Tremel, I. A. Dascalu, S. Shova and I. A. Gural'skiy, *Chem. – Eur. J.*, 2022, **28**, e202200924.
- 58 C. P. Berlinguette, A. Dragulescu-Andrasi, A. Sieber, J. R. Galán-Mascarós, H. U. Güdel, C. Achim and K. R. Dunbar, *J. Am. Chem. Soc.*, 2004, **126**, 6222–6223.
- 59 Y. Z. Zhang, D. F. Li, R. Clérac, M. Kalisz, C. Mathonière and S. M. Holmes, *Angew. Chem., Int. Ed.*, 2010, **49**, 3752–3756.
- 60 J. Mercurol, Y. L. Li, E. Pardo, O. Risset, M. Seuleiman, H. Rousselière, R. Lescouëzec and M. Julve, *Chem. Commun.*, 2010, **46**, 8995–8997.
- 61 D. Siretanu, D. F. Li, L. Buisson, D. M. Bassani, S. M. Holmes, C. Mathonière and R. Clérac, *Chem. – Eur. J.*, 2011, **17**, 11704–11708.
- 62 L. Cao, J. Tao, Q. Gao, T. Liu, Z. C. Xia and D. F. Li, *Chem. Commun.*, 2014, **50**, 1665–1667.
- 63 C. Y. Zheng, J. P. Xu, Z. X. Yang, J. Tao and D. F. Li, *Inorg. Chem.*, 2015, **54**, 9687–9689.
- 64 C. Q. Jiao, Y. S. Meng, Y. Yu, W. J. Jiang, W. Wen, H. Oshio, Y. Luo, C. Y. Duan and T. Liu, *Angew. Chem., Int. Ed.*, 2019, **58**, 17009–17015.
- 65 Y. K. Yang, C. Q. Jiao, Y. S. Meng, N. T. Yao, W. J. Jiang and T. Liu, *Inorg. Chem. Commun.*, 2021, **130**, 108712.
- 66 L. Y. Meng, Y. F. Deng and Y. Z. Zhang, *Inorg. Chem.*, 2021, **60**, 14330–14335.
- 67 P. Y. You, R. J. Wei, M. Xie, G. H. Ning and H. Oshio, *Inorg. Chem. Front.*, 2022, **10**, 288–295.
- 68 D. P. Dong, J. Q. Xiao, P. F. Zhuang, H. Zheng, L. Zhao, C. He, T. Liu and C. Y. Duan, *Inorg. Chem. Commun.*, 2012, **21**, 84–87.
- 69 A. Mondal, Y. L. Li, M. Seuleiman, M. Julve, L. Toupet, M. Buron-Le Cointe and R. Lescouëzec, *J. Am. Chem. Soc.*, 2013, **135**, 1653–1656.
- 70 Y. Z. Zhang, P. Ferko, D. Siretanu, R. Ababei, N. P. Rath, M. J. Shaw, R. Clérac, C. Mathonière and S. M. Holmes, *J. Am. Chem. Soc.*, 2014, **136**, 16854–16864.
- 71 C. Mathonière, D. Mitcov, E. Koumoussi, D. Amorin-Rosario, P. Dechambenoit, S. F. Jafri, P. Sainctavit, C. C. D. Moulin, L. Toupet, E. Trzop, E. Collet, M. A. Arrio, A. Rogalev, F. Wilhelm and R. Clérac, *Chem. Commun.*, 2022, **58**, 12098–12101.
- 72 T. Liu, Y. J. Zhang, S. Kanegawa and O. Sato, *Angew. Chem., Int. Ed.*, 2010, **49**, 8645–8648.
- 73 T. Liu, D. P. Dong, S. Kanegawa, S. Kang, O. Sato, Y. Shiota, K. Yoshizawa, S. Hayami, S. Wu, C. He and C. Y. Duan, *Angew. Chem., Int. Ed.*, 2012, **51**, 4367–4370.
- 74 D. P. Dong, T. Liu, S. Kanegawa, S. Kang, O. Sato, C. He and C. Y. Duan, *Angew. Chem., Int. Ed.*, 2012, **51**, 5119–5123.
- 75 J. X. Hu, L. Luo, X. J. Lv, L. Liu, Q. Liu, Y. K. Yang, C. Y. Duan, Y. Luo and T. Liu, *Angew. Chem., Int. Ed.*, 2017, **56**, 7663–7668.
- 76 Y. B. Huang, J. Q. Li, W. H. Xu, W. W. Zheng, X. P. Zhang, K. G. Gao, T. C. Ji, T. Ikeda, T. Nakanishi, S. Kanegawa, S. Q. Wu, S. Q. Su and O. Sato, *J. Am. Chem. Soc.*, 2024, **146**, 201–209.